Lecture 10 Particle Astrophysics
Gravitational Waves

Gravitational Waves

Imagine that we have a small perturbation to the metric:

$$g_{\mu\nu} = \eta_{\mu\nu} + h_{\mu\nu}, \qquad |h_{\mu\nu}| \ll 1.$$

After a lot of algebra, we can derive the following equation (to first order in $h_{\mu\nu}$

$$\Box^2 h_{\mu\nu} + \frac{1}{2} h^{\lambda}{}_{\nu,\mu\lambda} + \frac{1}{2} h^{\lambda}{}_{\mu,\nu\lambda} - \frac{1}{2} h^{\lambda}{}_{\lambda,\mu\nu} = 16\pi G S_{\mu\nu},$$

where,

$$\Box^2 = \eta^{\alpha\beta} \frac{\partial}{\partial x^{\alpha}} \frac{\partial}{\partial x^{\beta}} \equiv \frac{\partial^2}{\partial t^2} - \nabla^2, \quad S_{\mu\nu} = T_{\mu\nu} - \frac{1}{2} g_{\mu\nu} T^{\lambda}_{\lambda}.$$

In General Relativity (as in Electromagnetism) we can choose coordinates (*i.e.* pick a gauge) to simplify the equations. A convenient choice is the harmonic gauage,

$$\frac{\partial h^{\mu}{}_{\nu}}{\partial x^{\mu}} = \frac{1}{2}\frac{\partial h^{\mu}{}_{\mu}}{\partial x^{\nu}}.$$

The wave equation then becomes

$$\Box^2 h_{\mu\nu} = 16\pi G S_{\mu\nu}.$$

In vacuum ($S_{\mu\nu} = 0$) there are plane wave solutions

$$h_{\alpha\beta} = A_{\alpha\beta}\mathrm{exp}(ik_{\mu}x^{\mu}) + A^{*}_{\alpha\beta}\mathrm{exp}(-ik_{\mu}x^{\mu}).$$

The matrix $A_{\alpha\beta}$ is symmetric and has 10 independent components. After a lot of algebra, imposing the harmonic gauge condition, we can show that for a wave travelling in the x direction the physically distinct amplitudes are:

$$h_{\mu\nu} = \begin{pmatrix} 0 & 0 & 0 & 0 \\ 0 & 0 & 0 & 0 \\ 0 & 0 & h_{22} & h_{32} \\ 0 & 0 & h_{32} & -h_{22} \end{pmatrix}.$$

Now lets look at geodesic motion in the weak field limit:

$$\frac{D^2y}{D\tau^2} = -\frac{1}{2}(h_{22,00}y + h_{23,00}z),$$
$$\frac{D^2z}{D\tau^2} = -\frac{1}{2}(h_{23,00}y - h_{22,00}z).$$

If we have only an h_{22} mode ($+$ mode):

$$\frac{D^2y}{D\tau^2} = -\frac{1}{2}h_{22,00}y, \qquad \frac{D^2z}{D\tau^2} = \frac{1}{2}h_{22,00}z,$$

and if we have only an h_{32} mode ($\times$ mode):

$$\frac{D^2y}{D\tau^2} = -\frac{1}{2}h_{32,00}y, \qquad \frac{D^2z}{D\tau^2} = -\frac{1}{2}h_{32,00}z,$$

and the motion of test particles is as shown on the next page.

Note that the combinations $h_{22} \pm ih_{32}$ transform as $e^{\pm i2\theta}$ under spatial rotations – gravitational waves have *helicity* of ± 2. (Compare with photons).

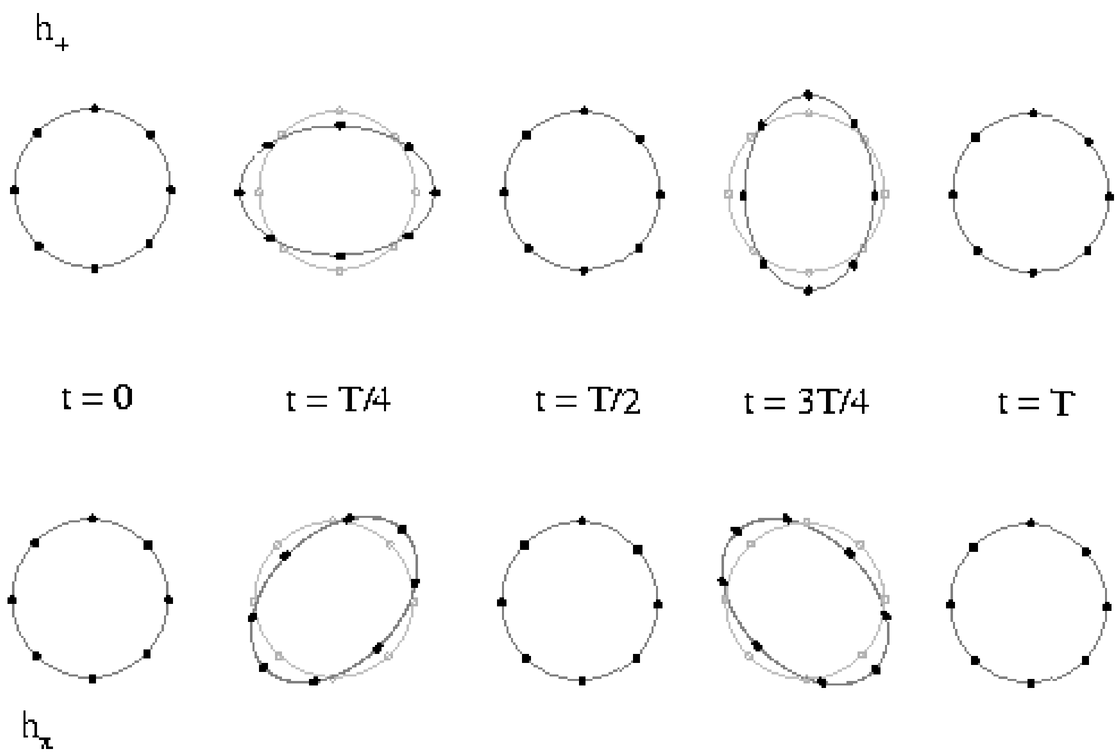

Figure I.1: The effect of a gravitational wave on a ring of free particles. The wave direction is perpendicular to the ring. The upper part shows the effect of a wave polarized on the + direction. The bottom figure shows the effect of a × polarized wave.

The Quadrupole Formula

Birkoff's theorem tells us that a spherically symmetric vacuum solution in GR must be static and asymptotically flat (*i.e.* described by the Schwarzchild metric). It therefore follows that a spherically symmetric pulsating object *cannot emit gravitational waves.*

For a slowly moving source, the loss of energy from gravitational radiation is give by the *quadrupole formula*:

$$L_{\mathrm{GW}} = \frac{1}{5}\langle \dddot{I}^{2} \rangle = \frac{1}{5}\langle \dddot{I}_{\alpha\beta} \dddot{I}^{\alpha\beta} \rangle,$$

where $I_{\alpha\beta}$ is the quadrupole:

$$I_{\alpha\beta} = \int \rho \left(x_\alpha x_\beta - \frac{1}{3}\delta_{\alpha\beta} r^3 \right) d^3\mathbf{x}.$$

Taylor-Hulse Binary Pulsar PSR 1913+16

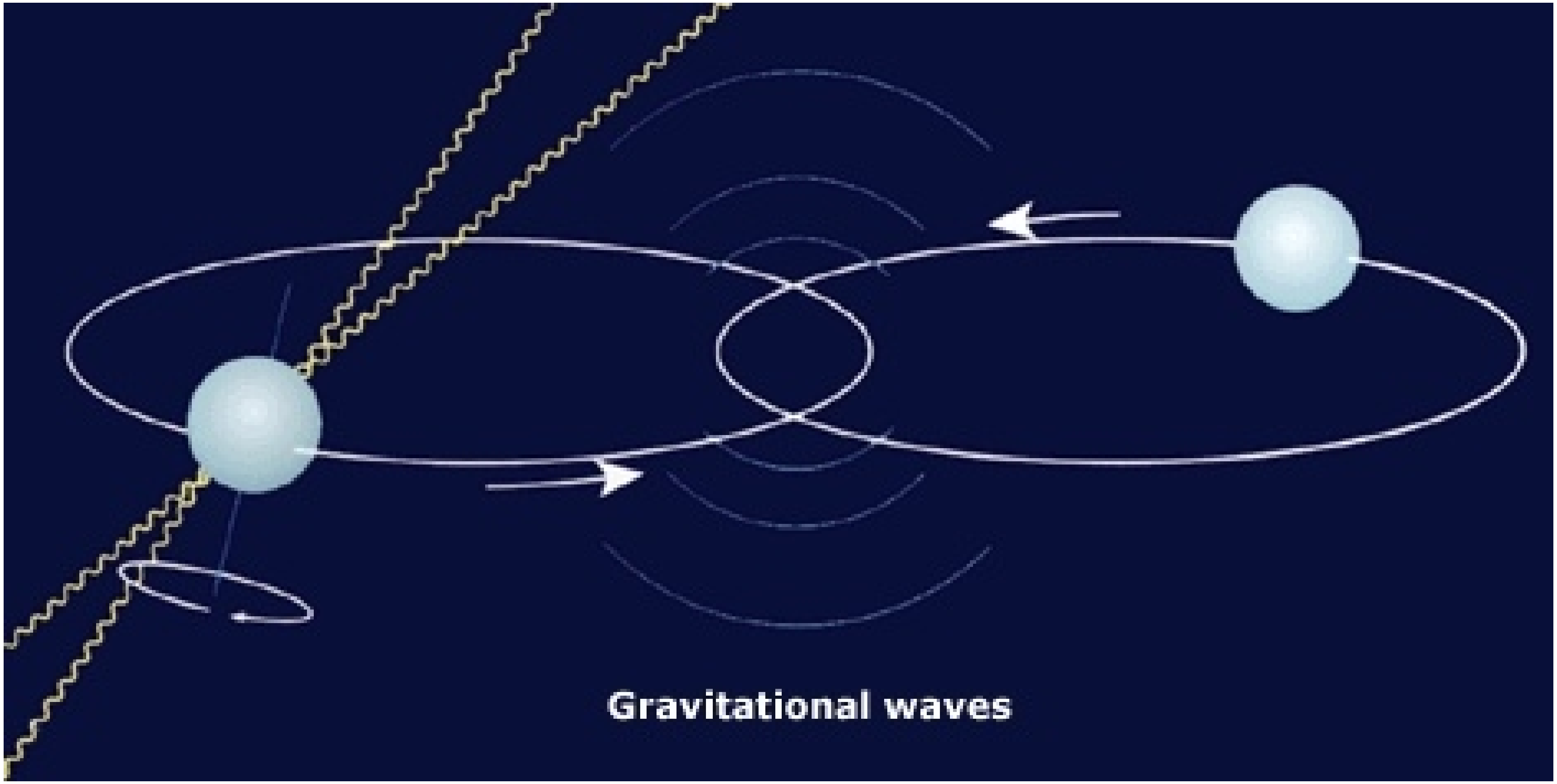

Binary period	=	7.751939337 hours
Pulsar period	=	59 milliseconds
Neutron star mass M_1	=	$1.4411(7)M_\odot$
Neutron star mass M_2	=	$1.3874(7)M_\odot$
Orbital eccentricity e	=	0.617

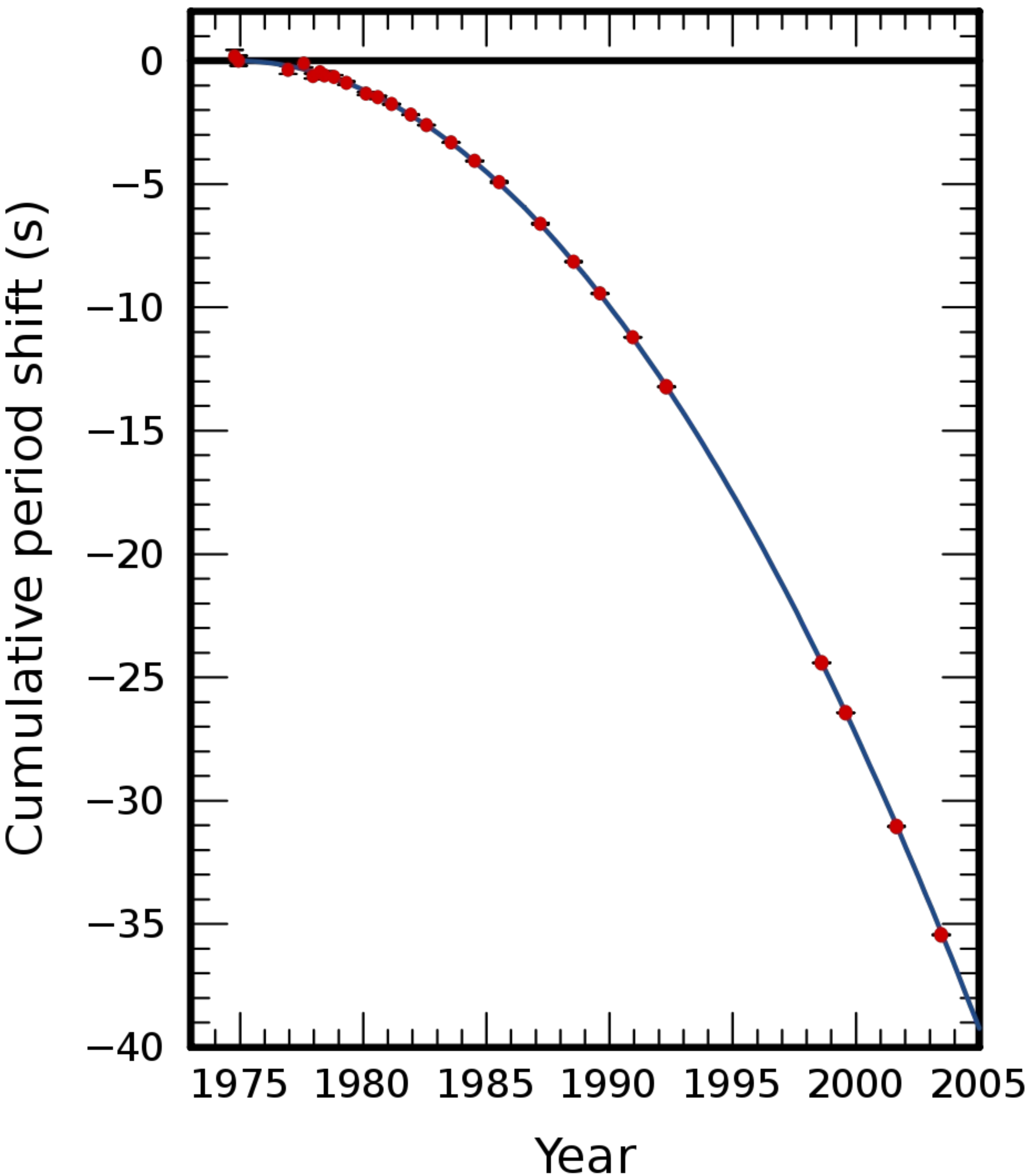

Period shifts by 80μs every 7.75 hours. The decrease in the period is *consistent with the predictions of GR* with a steady decrease in the orbital period

$$\frac{d\tau_{\text{orbit}}}{dt} = 2.4 \times 10^{-12}.$$

This is an (indirect) *detection of gravitational waves* .

Why should we try to detect gravitational waves?

- Fundamental tests of gravity: Do gravitational waves travel at the speed of light? Is the graviton massless? Scalar/tensor theories ....?

- Testing strong-field gravity: (Primarily via extreme mass-ratio inspirals (EMRIs). Are there 'naked singularities' (Kerr metric with $J/M > 1$). Deviations from the Kerr metric? Evidence for higher dimensional physics ....?

- Astrophysical objects: Nature of pulsars, formation of super-novae. How do supermassive black holes form? What is their abundance and angular momentum distribution as a function of time?

- Binary inspirals are standard candles. Can we use gravitational waves to constrain the Hubble constant, or dark energy?

- New sources: Gravitational radiation from cosmic strings? Stochastic background from inflation, or reheating, or first order phase transitions in the Early Universe? Background arising from new physics, *e.g.* nearby brane, or brane-bulk interactions ...?

Laser Interferometer Gravitational Wave Observatory (LIGO)

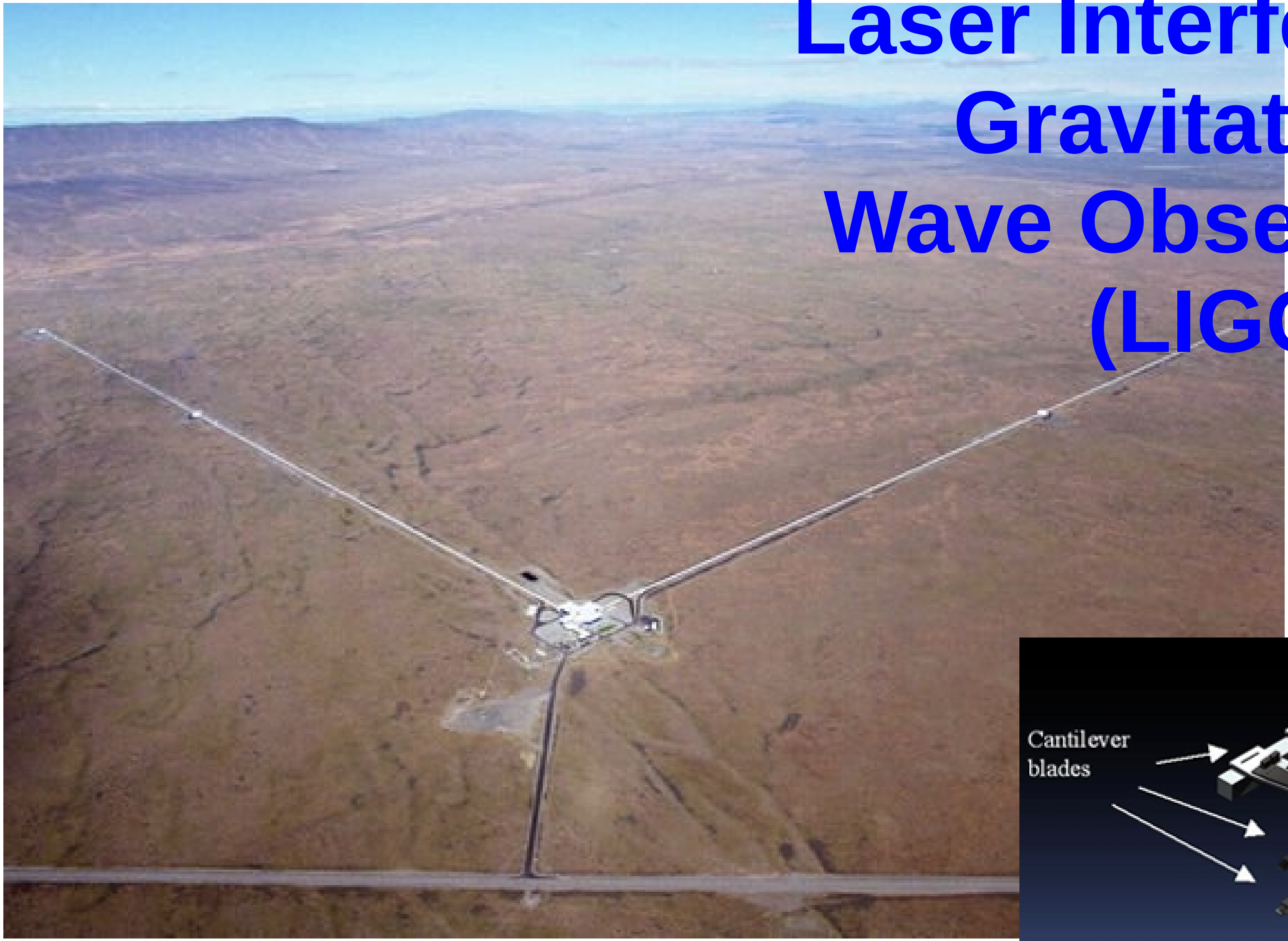

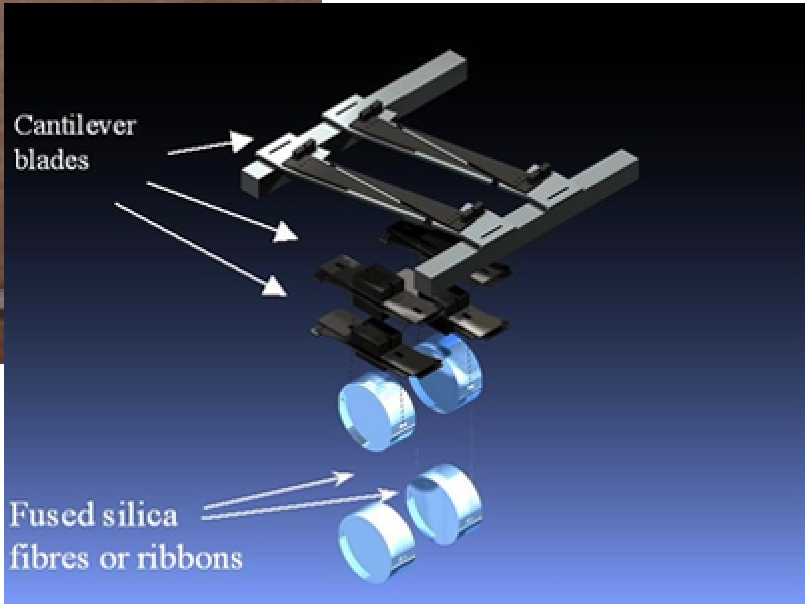

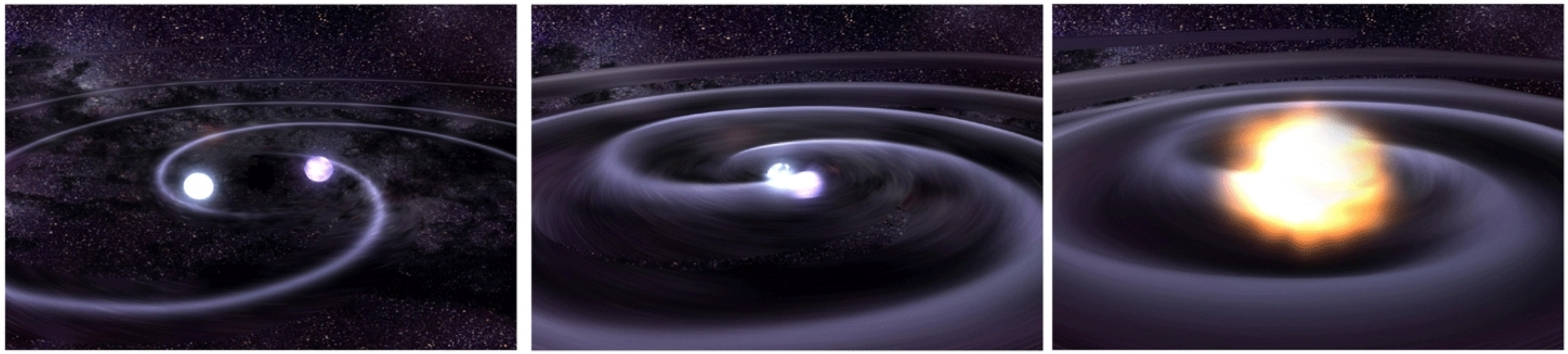

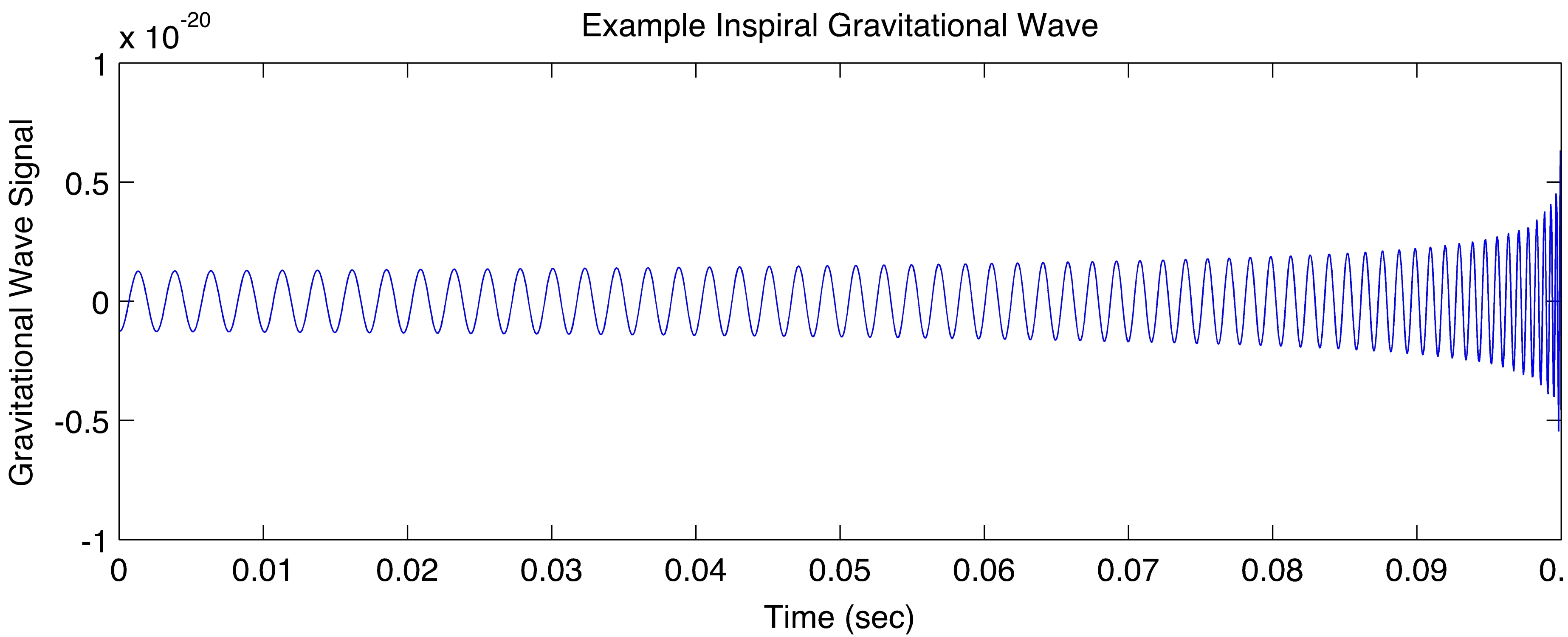

Example Inspiral Gravitational Wave
x 10^-20
1
0.5
0
-0.5
-1
Gravitational Wave Signal
0
0.01
0.02
0.03
0.04
0.05
0.06
0.07
0.08
0.09
0.1
Time (sec)

From Abbott etal 2009, Rep. Prog. Phys. 72, 076901.

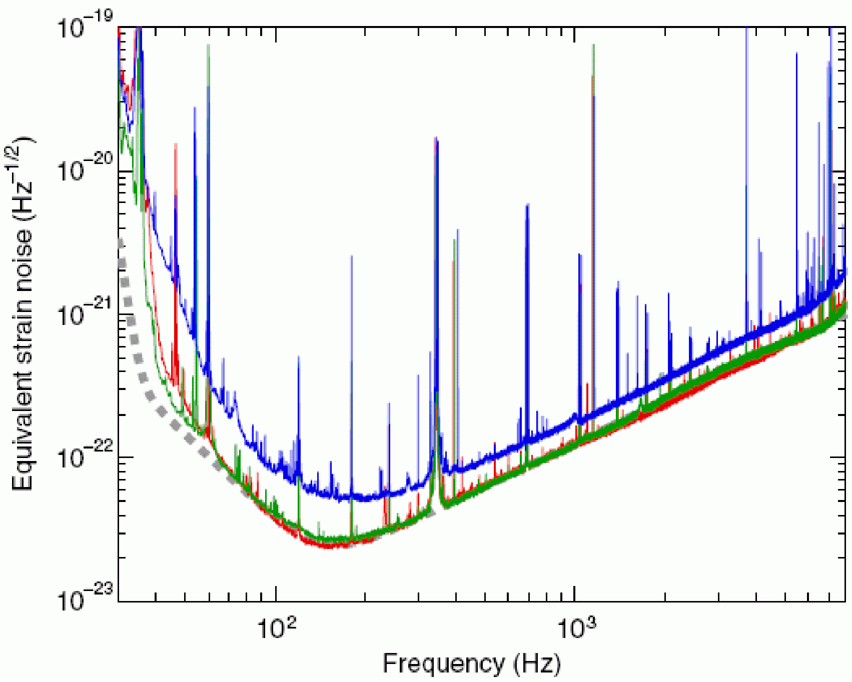

Figure 6. Strain sensitivities, expressed as amplitude spectral densities of detector noise converted to equivalent GW strain. The vertical axis denotes the rms strain noise in 1 Hz of bandwidth. Shown are typical high sensitivity spectra for each of the three interferometers (red: H1; blue: H2; green: L1), along with the design goal for the 4 km detectors (dashed gray).

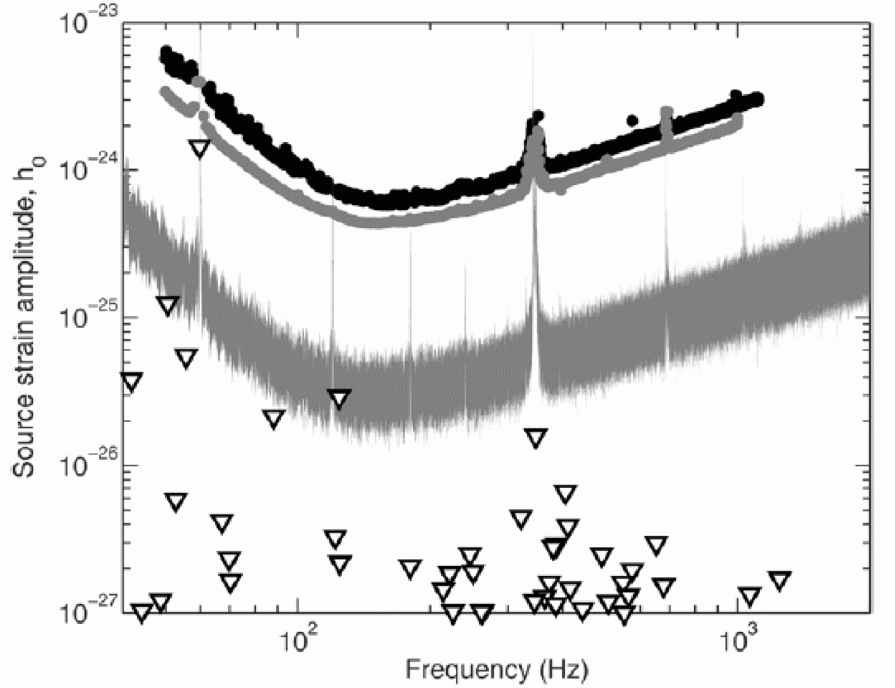

Figure 13. Limits on GW strain from rotating NSs. Upper curve (black points): all-sky strain upper limits on unknown NSs for spin-down rates as high as 5×10^{-9} Hz s^{-1} and optimal orientation, from analysis of the first 8 months of S5 data [89]. Middle curve (gray points): expected sensitivity for the Einstein@Home search with 5280 h of S5 data. Lower curve (gray band): expected range for 95% confidence level Bayesian upper limits on radio pulsars with known epherimides, using the full S5 data. Black triangles: upper limits on GW emission from known radio pulsars based on their observed spin-down rates.

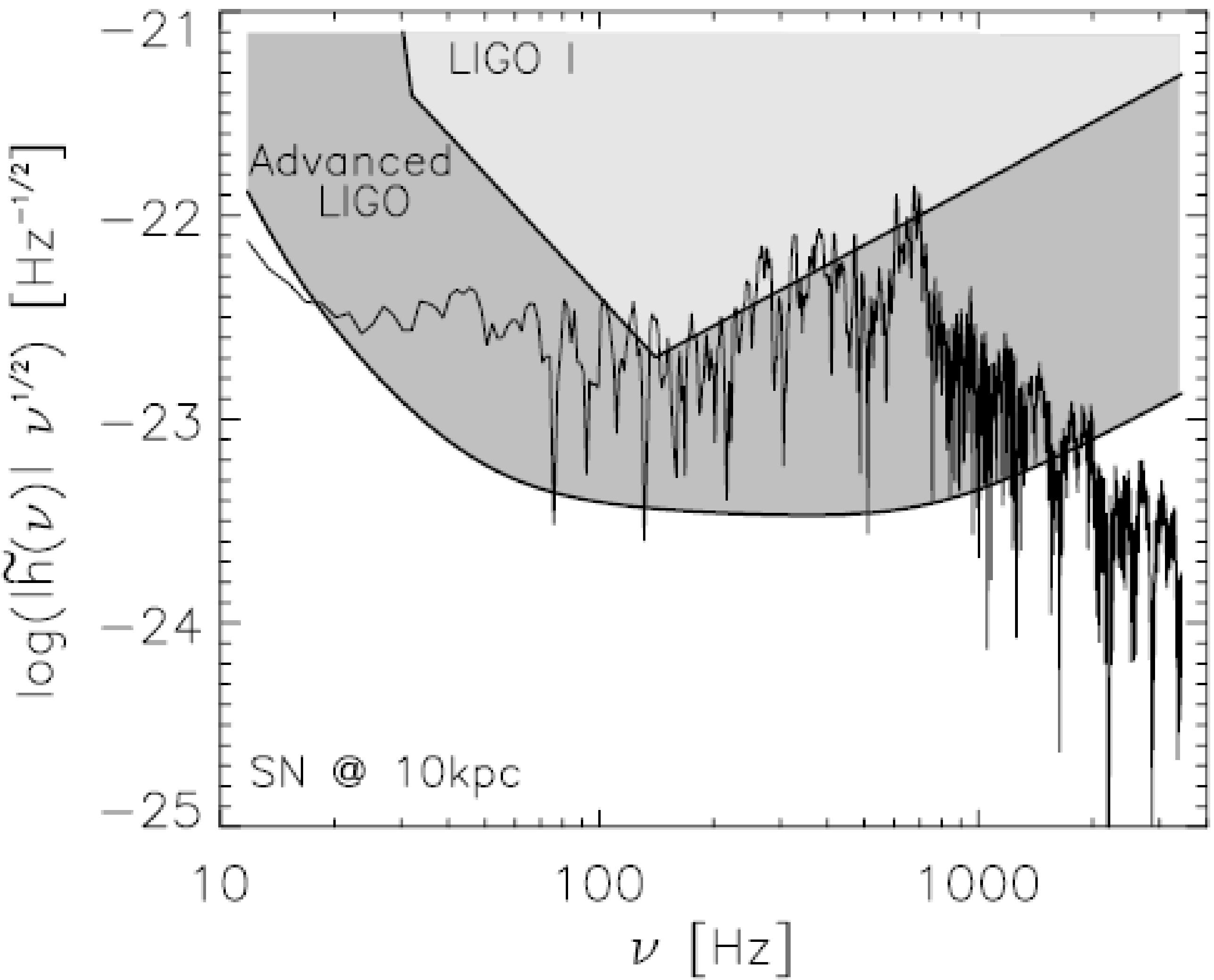

Gravitational wave strain spectrum from stellar collapse.

Laser Interferometer Space Antenna (LISA)

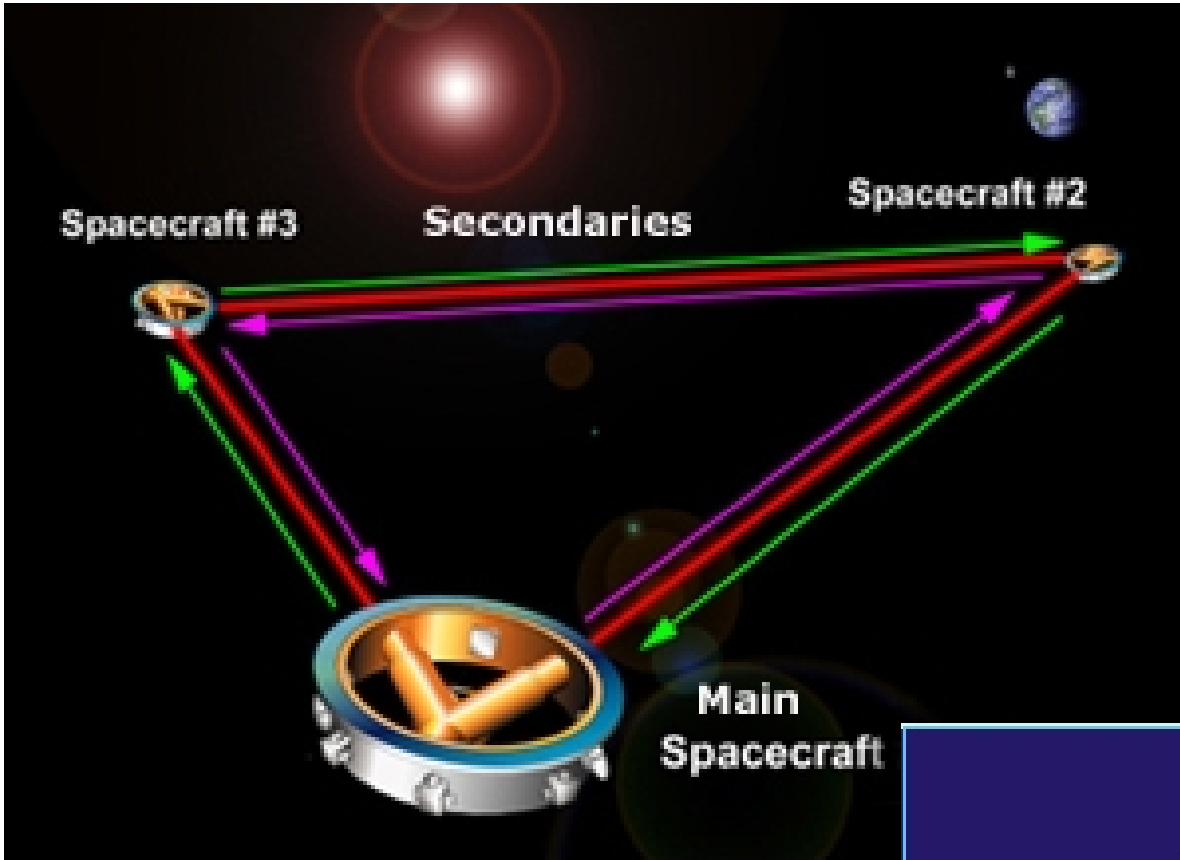

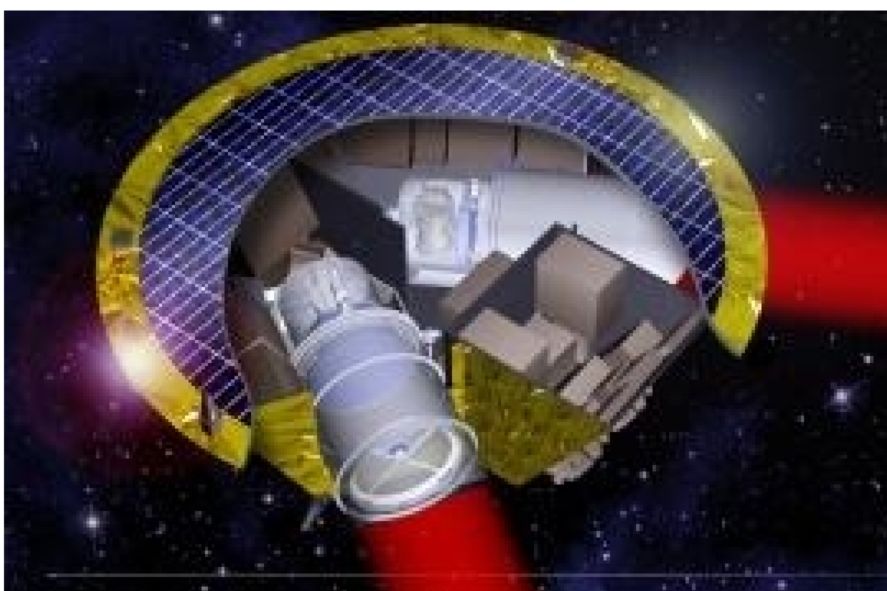

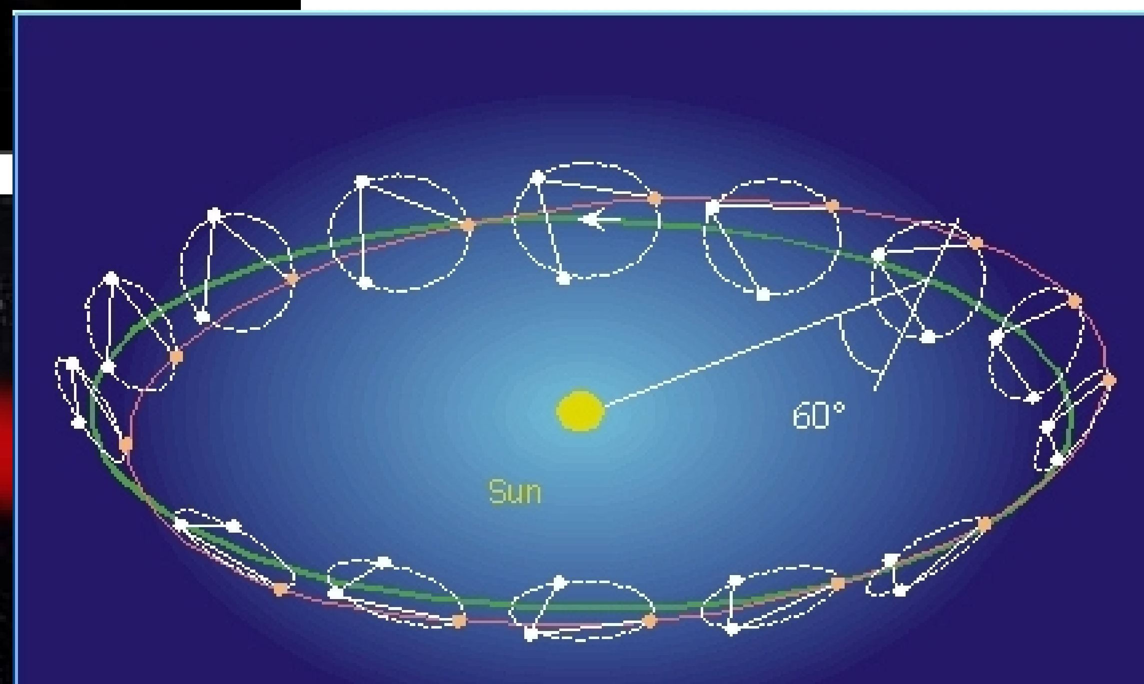

5 m km baseline, orbit 1 au from Sun

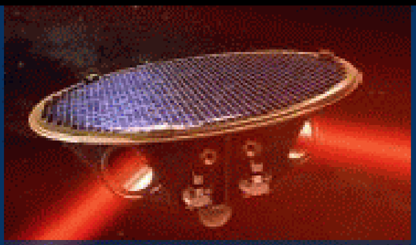

eLISA/NGO

LISA Pathfinder

Paving the way!

eLISA/NGO is a new concept for observing gravitational waves in space.

eLISA/NGO (**e**volved **L**aser **I**nterferometer **S**pace **A**ntenna/**N**ew **G**ravitational Wave **O**bservatory) will add a new sense to our perception of the Universe - for the first time we will observe e.g. Black holes and Neutron stars directly and gain unique information about the behaviour, structure and early history of the Universe.

eLISA/NGO will open the gravitational wave window in space and measure gravitational radiation over a broad band of frequencies, from about 0.1 mHz to 100 mHz, a band where the Universe is richly populated by strong sources of gravitational waves.

eLISA/NGO consists of one mother- and two daughter spacecraft separated by a distance of 1 Mio km, forming the first Michelson interferometer in space.

The entire mission will be a European-only mission and stay within resources available in Europe.

eLISA in NASA

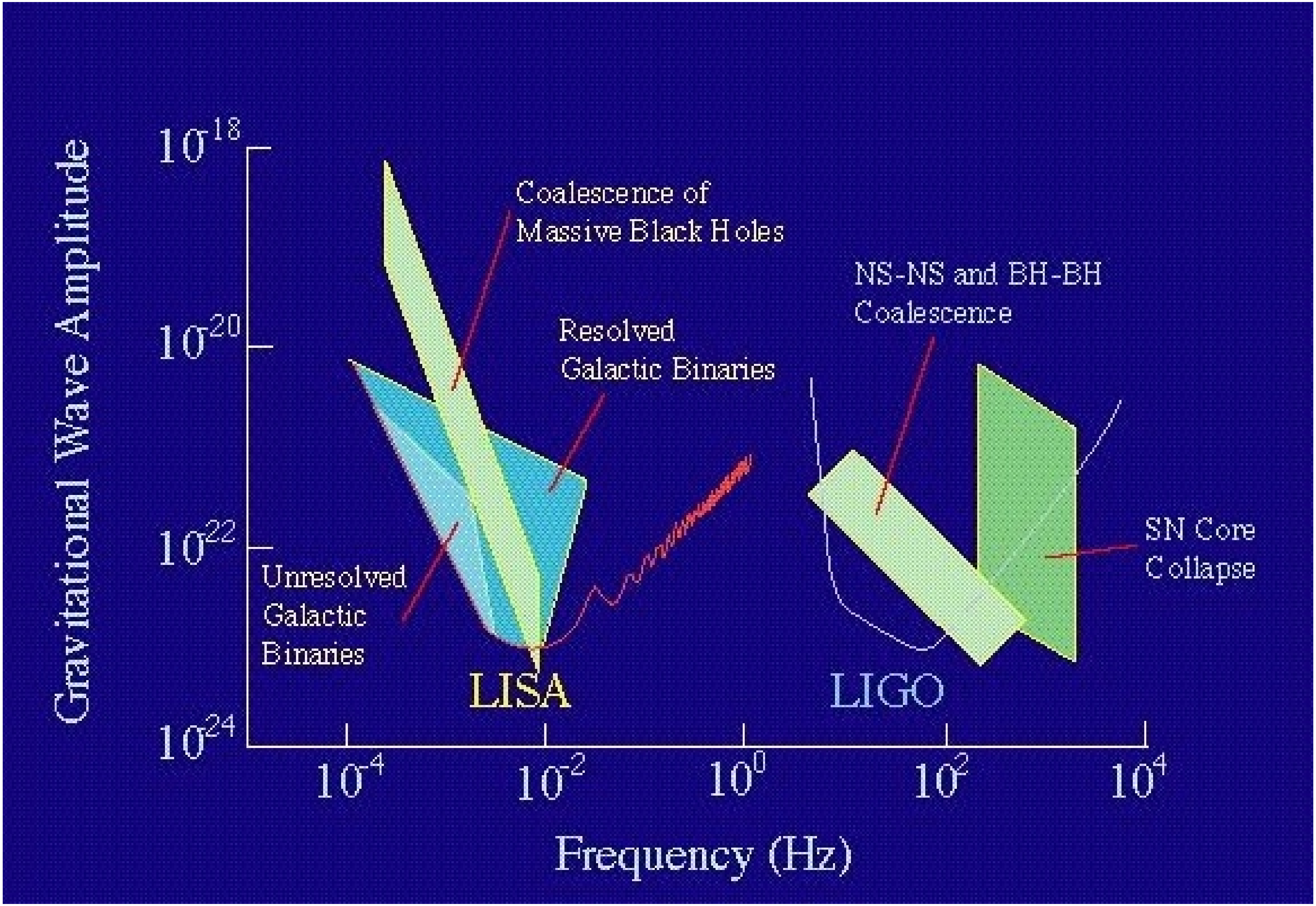

Gravitational Wave Amplitude
10^18
10^20
10^22
10^24
Coalescence of
Massive Black Holes
Resolved
Galactic Binaries
Unresolved
Galactic
Binaries
NS-NS and BH-BH
Coalescence
SN Core
Collapse
LISA
LIGO
10^-4
10^-2
10^0
10^2
10^4
Frequency (Hz)

Gravitational radiation from cosmic strings: From Damour abd Vilenkin 2005, PRD. 71, 063510.

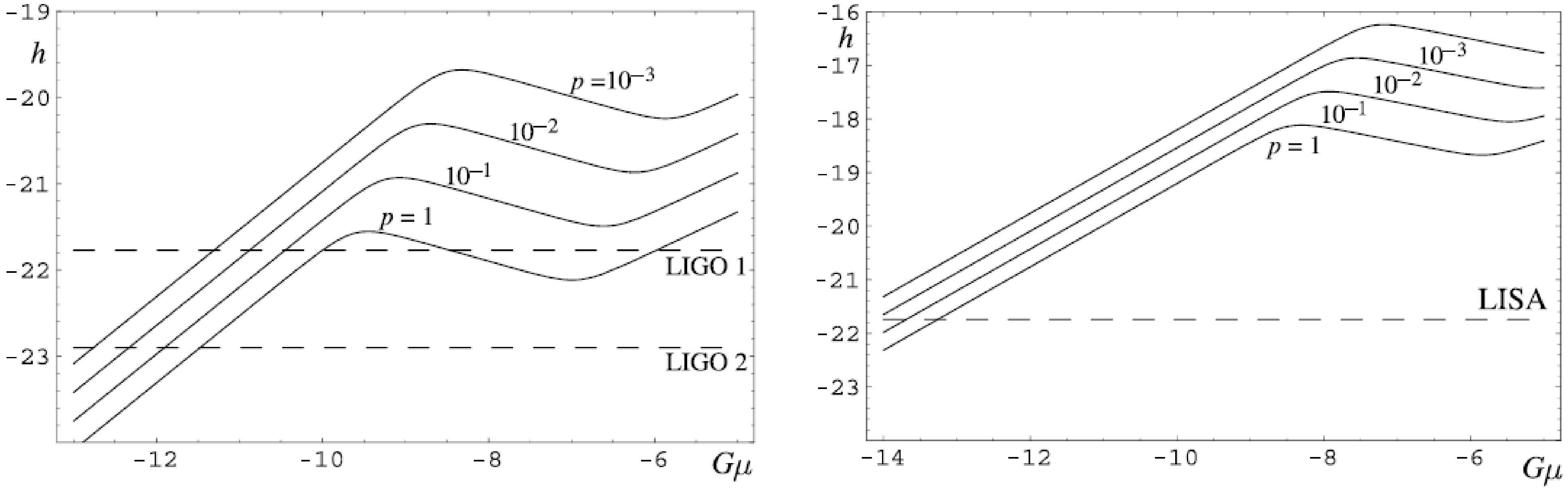

Stochastic gravitational wave background from inflation

Perturbations of FRW metric:

$$ds^2 = dt^2 - R^2(t)(\delta_{ij} + h_{ij})dx^i dx^j.$$

The tensor power spectrum observed today is given by

$$P_T(k) = \frac{32k^3}{\pi m_{\mathrm{Pl}}^2} \sum_{\lambda=+,\times} \langle h_\lambda^*(k, t_0) h_\lambda(k, t_0)\rangle.$$

The Einstein field equations tell us that each state h_λ evolves according to the massless Klein-Gordon equation

$$\frac{d^2 h_\lambda}{d\tau^2} + \frac{2}{R}\frac{dR}{d\tau}\frac{dh_\lambda}{d\tau} + k^2 h_\lambda = 0, \quad d\tau = \int dt/R(t), \qquad (1)$$

The tensor power spectrum at the end of inflation, $P_T(k, \tau_{\mathrm{inf}})$, is related to the present day tensor power spectrum via the solution of (1):

$$P_T(k,\tau_0) = T^2(k,\tau_0) P_T(k,\tau_{\mathrm{inf}}),$$

where

$$T(k,\tau_0) \approx \frac{3j_1(k\tau_0)}{k\tau_0}\sqrt{1 + 1.36\left(\frac{k}{k_{\mathrm{equ}}}\right) + 2.5\left(\frac{k}{k_{\mathrm{equ}}}\right)^2},$$

and $k_{\mathrm{equ}} = 0.073\Omega_m h^2 \mathrm{Mpc}^{-1}$ is the wavenumber corresponding to the Hubble radius at the time that matter and radiation have equal densities.

From the T_{00} component of the energy momentum tensor

$$T_{\mu\nu} = \frac{m_{\mathrm{Pl}}^2}{32\pi^2}\langle h_{ij,\mu} h_\nu^{ij}\rangle,$$

we can infer that *stochastic gravitational waves* from inflation contribute

$$\Omega_{\rm gw}(k) \approx \frac{15}{16 H_0^2 k_{\rm equ}^2 \tau_0^4} P_T(k, \tau_{\rm inf}) \approx 4.4 \times 10^{-15} h^{-2} r \left(\frac{f}{3 \times 10^{-18} {\rm Hz}} \right)^{n_T},$$

where r is the tensor-scalar ratio and n_T is the tensor spectral index.

Prospects for detecting scale-invariant inflationary tensor modes

Experiment	$\Omega_{\rm gw} h^2$ limit	freq. (Hz)	r limit	$V^{1/4}$ (GeV)
Planck	–	–	~ 0.05	1.5×10^{16}
CMBpol	–	–	10^{-3}	6×10^{15}
Advanced LIGO	10^{-9}	100	2×10^5	–
LISA	10^{-11}	0.005	2×10^3	–
BBO/DECIGO	$\sim 10^{-17}$	0.1	2×10^{-3}	7.2×10^{15}
Ultimate DECIGO	10^{-20}	0.1-1.0	2×10^{-6}	1.3×10^{15}

Gravitational waves from reheating

Suppose we couple the inflaton ϕ with a second (scalar) field χ. We will assume the 'toy' Lagrangian:

$$\mathcal{L} = \frac{1}{2}\partial_\mu\phi\partial^\mu\phi + \frac{1}{2}\partial_\mu\chi\partial^\mu\chi - \frac{1}{2}m^2\phi^2 - \frac{1}{2}g^2\phi^2\chi^2.$$

The equation of motion for χ is

$$\ddot{\chi} + 3H\dot{\chi} - \frac{1}{R^2}\nabla^2\chi + g^2\phi^2\chi = 0.$$

So, expanding χ in Fourier (momentum) modes:

$$\ddot{\chi}_k + 3H\dot{\chi}_k + \left(\frac{k^2}{R^2} + g^2\phi^2\right)\chi_k = 0. \qquad (2)$$

At the end of inflation, let's assume that ϕ oscillates rapidly with a time-averaged amplitude Φ and let's ignore the expansion of the Universe. If we then make the variable changes:

$$q = \frac{g^2 \Phi^2}{4m^2}, \quad A = \frac{k^2}{m^2} + 2q, \quad z = mt,$$

equation (2) is seen to be a *Mathieu equation*

$$\frac{d^2 \chi_k}{dz^2} + (A - 2q \cos(2z))\chi_k = 0,$$

which has solutions

$$\chi_k \propto f(z) \exp^{\pm i \mu z},$$

where $f(z)$ is periodic. If the Mathieu exponent μ has an non-zero imaginary value, the χ field will grow exponentially – there is a *parametric resonance* favouring the production of certain momentum modes.

The χ field can become extremely inhomogeneous, leading to the generation of gravitational waves after inflation.

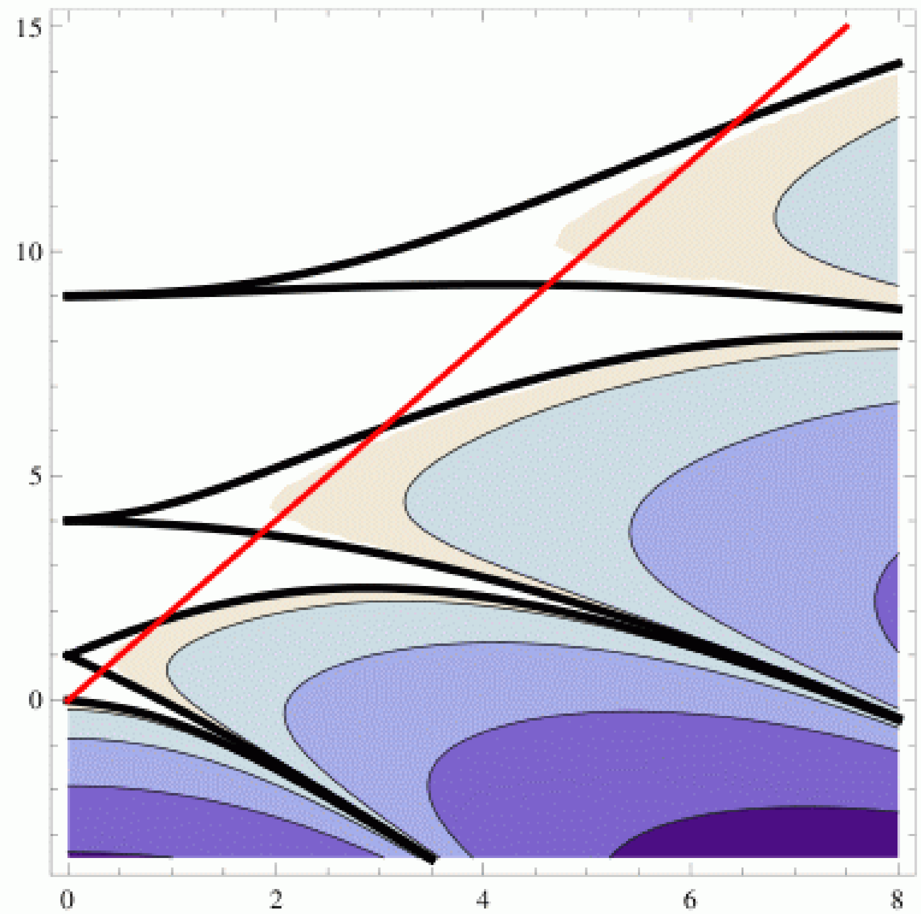

Figure 1. The imaginary part of the Mathieu critical exponent is plotted, with darker colors corresponding to a larger imaginary component. Outside the heavy black lines the exponent is real-valued, and the corresponding solutions are strictly oscillatory. The diagonal line corresponds to $A = 2q$.

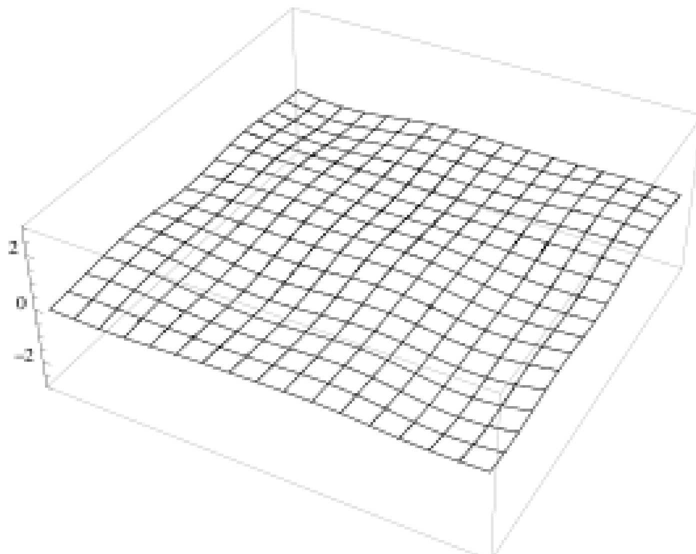

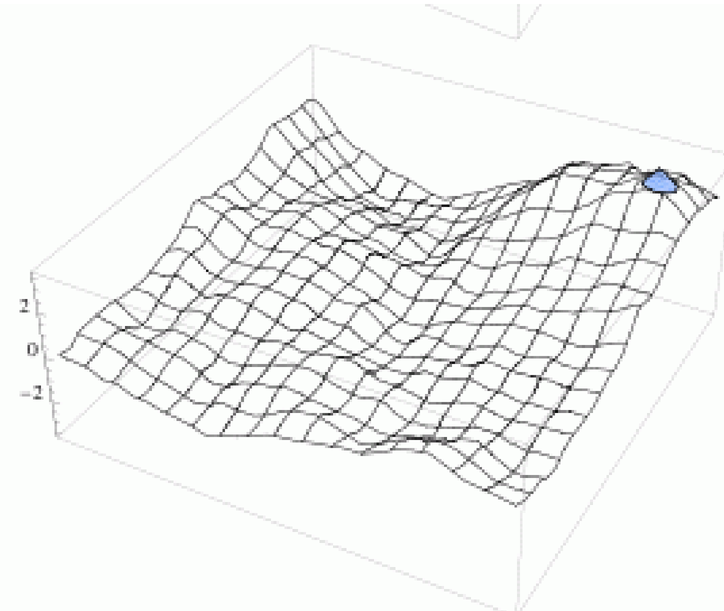

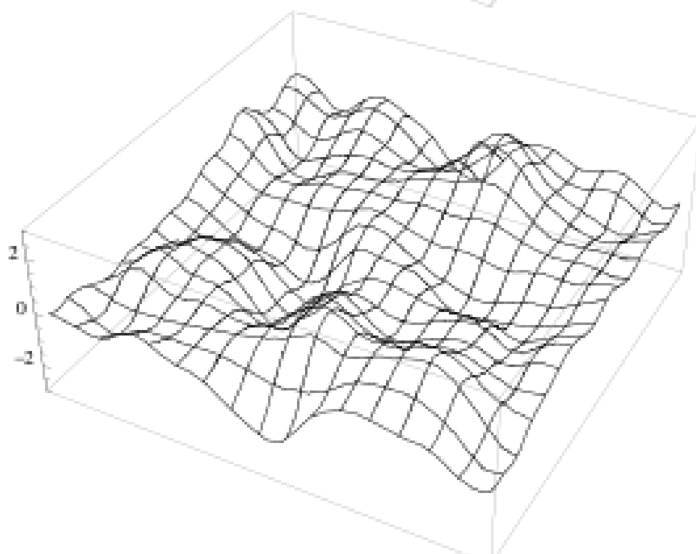

Figure 2. A cross section of the χ field at three times, with an arbitrary normalization. Gravitational waves are induced by (time varying) spatial gradients, which peak in the middle frame.

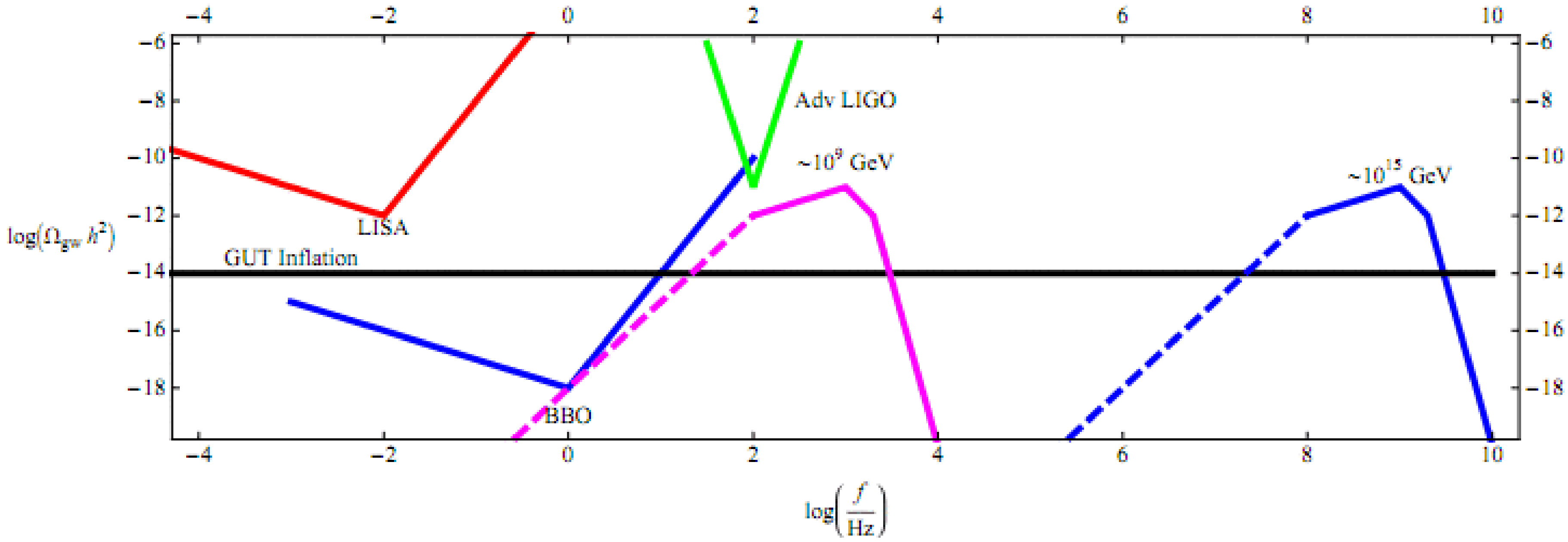

FIG. 2: We sketch the gravitational wave spectra obtained for the lowest and highest energy models computed here, relative to that of the Advanced LIGO goal, and the proposed LISA and BBO experiments. We see that inflationary models with lower energy scale may lead to a signal which is visible at LIGO scales if the sensitivity of LIGO is further improved, and with BBO. The tensor background generated by quantum fluctuations during GUT scale inflation is shown by the solid horizontal line. The dashed lines denote the inferred k^3 tails. The spectra generated by the inflationary scenarios considered in [5, 15] roughly overlap with the 10^{15} GeV spectrum depicted above.

International Pulsar Timing Array

(see e.g. Dobbs etal Class. Quantum Gravity, 2010, 27, 084013)

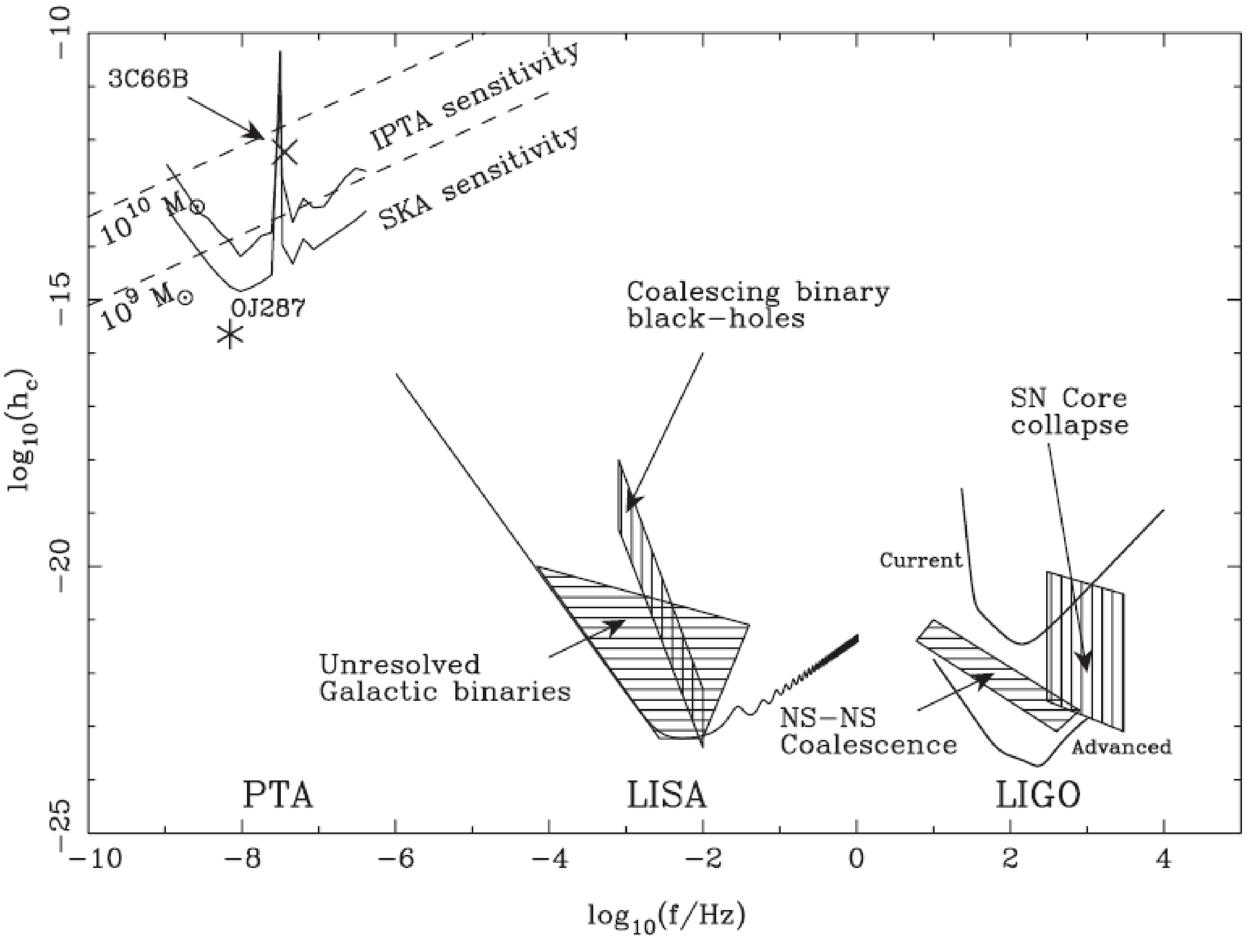

Figure 4. The sensitivity to individual sources of GWs is shown for the IPTA and a possible future experiment with the SKA. The expected signals from coalescing blackholes at the cores of 3C66B and OJ287 are shown. The dashed lines indicate the expected signals from black-hole binary systems with chirp masses of 10^9 and 10^{10} $M_\odot$ respectively, situated in the Virgo cluster. For comparison, the sensitivity curves of LIGO and LISA and predicted signal levels are also shown.